DESIGN AND WORKING PERFORMANCE STUDY OF A NOVEL MICRO PARALLEL PLATE COMBUSTOR WITH TWO NOZZLES FOR MICRO-THERMOPHOTOVOLTAIC SYSTEM

by

Jianfeng PAN [*]***, Zhiyong HOU, Yangxian LIU, Aikun TANG, Jun ZHOU, Xia SHAO, Zhenhua PAN, and Qian WANG***

School of Energy Resources and Power Engineering, Jiangsu University, Zhenjiang, China

Original scientific paper
DOI: 10.2298/TSCI141109069P

Micro-combustors are a key component in combustion-driven micropower generators, and their performance is significantly affected by their structure. For the application of micro-thermophotovoltaic system, a high and uniform temperature distribution along the walls of the micro-combustor is desired. In this paper, a 3-D numerical simulation has been conducted on a new-designed parallel plate micro-combustor with two nozzles. The flow field and the combustion process in the micro-combustor, and the temperature distribution on the wall as well as the combustion efficiency were obtained. The effects of various parameters such as the inlet angle and the fuel volumetric flow rate on the performance of the micro-combustor were studied. It was observed that a swirl formed in the center of the combustor and the radius of the swirl increased with the increase of the inlet rate, and the best working condition was achieved at the inlet angle, $\theta = 20°$. The results indicated that the two-nozzle combustion chamber had a higher and more uniform mean temperature than the conventional combustor under the same condition.

Key words: *micro-combustion, two-nozzle combustor, inlet angle, swirl, temperature distribution*

Introduction

The demand for light-weight and long-life micro-power sources is emerging with the miniaturization of electromechanical devices [1-4], leading to the development of combustion-based micropower generators [5-7]. The advantage of the combustion-based micropower generators is much higher energy density than conventional energy systems. Thus, since the pioneering work of micro gas turbines by Epstine and Senturia [8], several concepts of micro power generators have been developed, such as the micro-electromechanical systems (MEMS) rotary engine [9], the micro free-piston engine [10], and the micro-thermophotovoltaic (MTPV) systems [11, 12]. The MTPV power generator currently developed around the world is a kind of micro power device [11]. For the practical application of the micro-combustion, there are still several challenges needed to be overcome to achieve high performance micro-combustion. One problem is that the reduced size of the combustor leads to a dramatic increase in the combustor surface to volume ratio, which subsequently leads to a significant heat loss and radical destruction on the combustion wall. Another problem is the short fuel residence time in the mi-

* Corresponding author; e-mail: mike@ujs.edu.cn

cro-combustor, which causes blow-off phenomenon and low combustion efficiency. The MTPV is an ideal way to realize the miniaturization of a power source package that will meet the requirements of MEMS. It has no moving parts, is highly robust and reliable, and is suitable for use in commercial electronics and personal micro devices. The high surface area to volume ratio of micro combustor holds the promise for the MTPV power generator to achieve a high power density [13]. Previous works show that it is particularly important to develop combustors that can efficiently convert fuel into usable radiation energy for thermophoto-voltaic (TPV) utilization [14, 15]. Thermal emitters must withstand high temperatures (~1400 °C) and be durable [16], and the temperature distribution must be uniform. The MTPV uses photovoltaic (PV) cells to convert heat radiation, from the combustion of fossil fuels, into electricity. When the wall, *i.e.* the emitter, is heated to a sufficiently high temperature, the heated wall emits photons. It is well known that only photons with energy greater than the bandgap of PV cells can evoke free electrons and generate electricity under the function of p-n junction formed in PV cells. Thus, the high temperature of the wall is needed to emit utilizable photons. However, with the conventional micro-combustor is difficult to get high and uniform temperature distribution. The high temperature can only be obtained on the inlet side, which is not good for the application of the MTPV and low combustion efficiency. Therefore, different experimental and numerical investigations have been done until now to optimize the conventional design. The method which uses the Swiss-roll type heat exchanger called excess heat excess enthalpy burners [17] is used to improve the performance of the micro-combustor. In an excess enthalpy combustor, combustion products and pre-mixed reactants flow in adjacent channels in opposite directions. This configuration allows the unburned mixture to be preheated by the high-temperature exhaust gas and when the maximum flame temperature is augmented, therefore heat loss from walls decreases, the quenching cannot occur. So the flame becomes stronger [18, 19] and the flammability limits will be effectively extended. Chou and Yang [13] utilized porous media to enhance the heat transfer between the high temperature combustion products and the emitter wall, as well as to increase the temperature along the wall. Hydrogen-air swirling premixed flames micro-combustion were investigated using direct numerical simulation by Wang and Luo [20] and it was found that most of the flame elements lie in the laminar flame regime and the thin reaction zones regime. A numerical study on CH_4 and air premixed combustion inside a small tube with a temperature gradient at the wall was undertaken to investigate the effects of inlet velocity, equivalence ratio and combustor size on combustion characteristics by Feng and Liu [21] and it was concluded that increasing wall temperature is an effective way to stabilize a flame for a given combustor size.

The combustor structure significantly influences the stability limits of flame and the flame position, which will affect the performance of the micro-combustor. Khandelwal [22] experimentally studied the characterization of flame stability behavior in a 2.0 mm diameter micro-combustor with three backward facing steps, it was observed that the zone of re-circulation created due to the sudden expansion at the backward step aids in stabilizing the flame inside the micro-combustor and improved the limits of flame stability significantly. Fan and Wan [23] numerically investigated the effect of bluff body shape on the blow-off limit of hydrogen/air flame in a planar micro-combustor. They developed a micro-combustor with a triangular bluff body, which has a demonstrated five-time extension in the blow-off limit compared to straight channel. These studies show that the changes of combustion chamber structure can affect the movement of the gas flow, resulting in different combustion processes. Hence, it is believed that the research on the combustor structure, which can change the flow structure, is significant to improve the performance of the micro-combustor.

However, the structures of some of the combustion chambers are rather complex to be used for practical application. In order to achieve a higher and more uniform temperature distribution and an easily built combustor, a newly-designed type of micro-combustion parallel plate chamber with two nozzles is presented in this paper. In this paper, a 3-D numerical simulation has been conducted on a newly-designed parallel plate micro-combustor with two nozzles. The flow field and the combustion process in the micro-combustor, and the temperature distribution on the wall as well as the combustion efficiency are obtained. The effects of various parameters such as the inlet angle and the fuel volumetric flow rate on the performance of the micro-combustor are studied. The main contribution of this new combustor is that a swirl will form in the center of the combustor, which can extend the fuel residence time and improve the combustion efficiency. Moreover, the swirl combustion can expand the high temperature zone compared to the conventional type, which is beneficial when utilizing the MTPV system. The flow rate and the inlet angle, θ are varied to simulate the combustion characteristics.

Combustor models and boundary conditions

Combustion chamber and the mesh

The newly-designed micro-combustion chamber comprises two nozzles – combustor A (D = 10 mm, L = = 10 mm, H = 0.6 mm), two symmetrically arranged circular nozzles with r = = 0.25 mm, and only one circular outlet with R = 0.5 mm on the wall, as shown in fig.1(a). In contrast, fig. 1(b) shows a conventional micro-combustor named as combustor B with the same dimensions as combustor A.

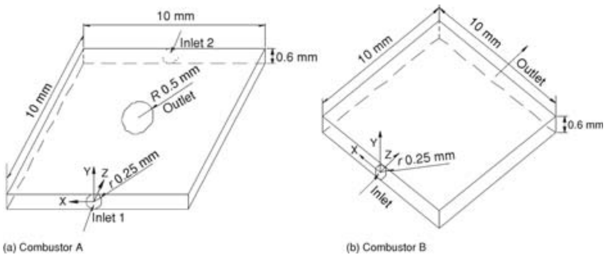

Figure 1. Structural model of combustors A and B

The origin is fixed at the center of the inlet plane. Premixed gas is the hydrogen-oxygen mixture with the equivalence ratio of 1.0. The wall material of the combustion chamber is SiC with a thermal conductivity of 92 W/mK, density of 3.10 g/cm^3 and emissivity of 0.77. Combustor A is meshed using mixed grid with the interval size 0.1. Considering the rule structure of combustor B, it is meshed using structured grid and the interval size is 0.1 as well. The grid number of combustors A and B are 473857 and 142200, respectively.

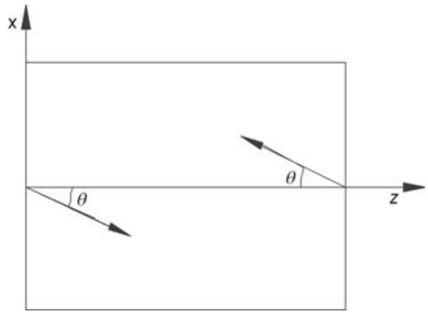

Figure 2. Schematic diagram of inlet angle θ

In combustor A, the inlet angle θ for the inlet gas flow is defined as the angle between the direction vector of inlet gas flow and z-axis as shown in fig. 2.

Governing equations

The governing equations of mass, chemical species, momentum, and energy are solved for steady low Mach number viscous flow. Thus, the four assumptions are made in the simulation [24]: (1) no Dufour effects; (2) no work done by pressure and viscous forces; and (3) steady-state flow. Based on these assumptions, the governing equations are to discretize using the finite-volume method and solved by ANASYS Fluent Release 14.0 [25]. The Reynolds number of the fluid flow ranges from approximately 212 when the flow rate is 400 sccm*, to 1060 when the flow rate is 2000 sccm for the simulated case; hence, the laminar finite rate model is employed. The radiation model is chosen to be discrete ordinates (DO) model. The fluid density is calculated by using the ideal law. The specific heat, viscosity, and the thermal conductivity of the fluid mixture are calculated using the mass weighted average method. First-order upwind scheme is used to discretize the governing equations, and simple algorithm is used to deal with the pressure-velocity coupling. Hydrogen-oxygen mixture reaction is modeled using the skeletal mechanism, which is composed of nine species and nineteen reaction steps [26]. Velocity inlet and pressure outlet are defined, respectively, as the inlet and outlet boundary conditions. Heat transfer from the wall of the combustor to the environment is also considered in this work.

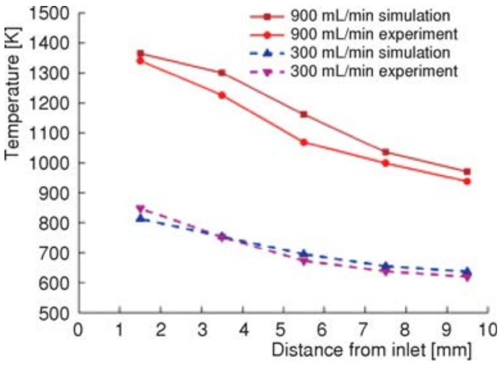

Figure 3. Experimental and numerical temperature distribution along the centerline of the conventional combustor wall

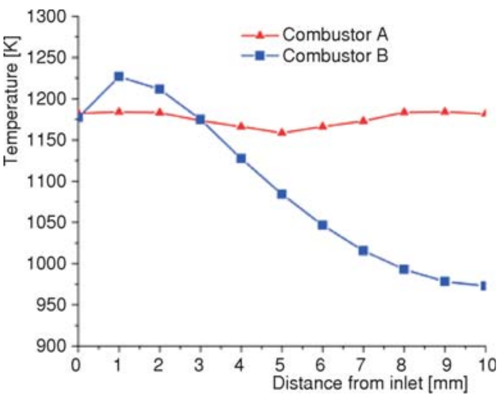

Figure 4. Average wall cross-section temperature distribution for combustors A and B

In our previous work, we investigated conventional combustor by using experimental as well as numerical simulation [27]. The governing equations have been used in the conventional combustor in numerical simulation and we found that the difference between the numerical and experimental results were less than 7%, which indicated numerical results agreed reasonably well with the experimental results on the temperature distribution in different inlet rates, as shown the temperature distribution of the wall along z-axis in fig. 3. This guarantees the accuracy of the numerical model adopted in this paper.

Results and discussion

Verifying the feasibility of the two-nozzle micro combustion chamber

In some micro power systems, such as MTPV and thermoelectric (TE) devices, the energy conversion rate depends on the uniformity of the temperature profiles on the wall. To investigate the feasibility of the two-nozzle micro combustor, an 800 sccm inlet flow rate is set in combustors A and B, the volumetric flow rate is 400 sccm for each nozzle for combustor A, with an inlet angle θ of 0°. The average temperature of the wall cross-section along the z axis is shown in fig. 4.

It can be seen from fig. 4 that with the same entire flow rate, the wall temperature distribution of combustor A is more uniform than that of combustor B. In the region of $z > 3$ mm, the average temperature of combustor A is higher

* sccm-standard cubic centimeters per minute

than that of B with a maximum difference around 210 K. So combustor A shows better feasibility than combustor B for MTPV system utilization.

Factors affecting combustion characteristic

Inlet angle θ

The inlet angle θ is taken as 0°, 10°, 20°, 30°, and 40°, respectively. When the hydrogen-oxygen mixture volumetric flow rate is 800 sccm, the central cross-section temperature distribution of x-z plane of combustor A is simulated and displayed in fig. 5 at different inlet angles. It can be seen from fig. 5 that the maximum temperature is 2235 K when θ = 20°, while the maximum temperature drops to 2011 K when the inlet angle is increased to θ = 40°. It can also be seen from fig. 5 that the shape of the flame and the location of the swirl changes in the combustor when θ changes. The flames are coaxial with an inlet angle θ = 0° as shown in fig. 5(a). The high-temperature region (with the red color) is only located in the center of the combustor within a small area, thus the average temperature in the combustor is the lowest. Similarly, as it can be observed in fig. 5, the flames deviate from the central axis of the combustor and the high-temperature region expands with the increase of inlet angle. Figure 5(c) shows that the high-temperature flame zone expands and the swirl forms in the center of the combustor when θ = 20°. In fig. 5(d), however, with the increase of inlet angle, the area of the high-intensified combustion region becomes smaller. This is because the unburned mixed gas coming from the inlet is closer to the shorter side of the combustor section which restricts the expansion of the flame. This trend becomes more obvious when θ = 40°, and the high-temperature region of the flame is smaller than when it is at θ = 30° with an associated reduction of the average wall temperature.

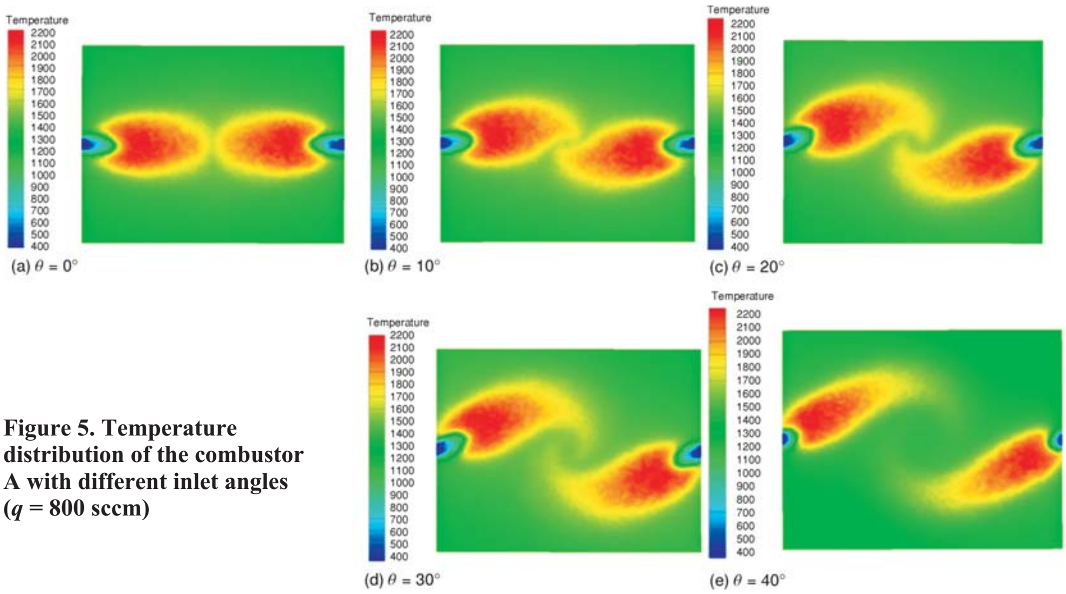

Figure 5. Temperature distribution of the combustor A with different inlet angles (*q* = 800 sccm)

From the presented results, it can be concluded that the mixed gas flow will shift towards the shorter side of the combustor section as inlet angle increases, which will cause the mixed gas to spread to different locations and ultimately change the temperature distribution within the combustion region. The average wall temperature for different inlet angles and flow

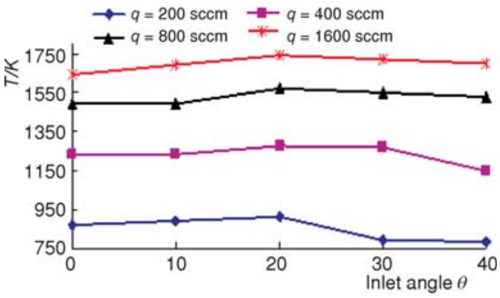

Figure 6. Average wall temperature with different inlet angles and flow rates

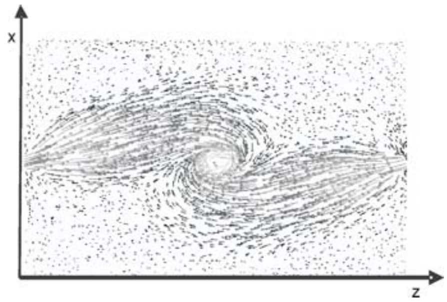

Figure 7. Map of the velocity vector in θ = 20° (q = 800 sccm)

rates is shown in fig. 6. It can be seen that the highest average temperature occurs at the inlet angle θ = 20° for different inlet flow rates. Therefore, it seems that the best working condition of the inlet is 20° for MTPV application.

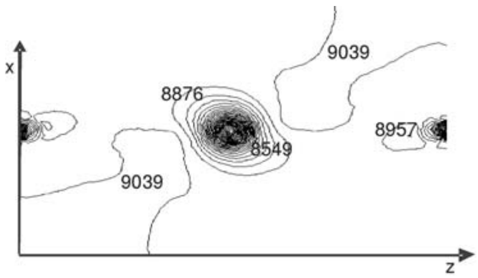

Figure 8. Map of the pressure nearby outlet in θ = 20° (q = 800 sccm)

With the change of the inlet angle θ, the combustion progress in the combustion chamber is affected for the following reason. Due to the inlet angle, a swirl forms in the combustor, the mixed gas molecules moves along with the swirl. This swirl makes the low pressure at the outlet. Therefore, the burning area is different when the inlet angle changes and the swirl lower the temperature of the central area in the combustor.

The velocity distribution of the mixture a flow rate of q = 800 sccm and inlet angle θ = 20° is presented in fig. 7. The pressure distribution near the outlet of the combustor is shown in fig. 8. It can be verified from fig. 8 that a large pressure gradient exists near the outlet with a pressure of 5140 Pa at the center. At the same time, the maximum pressure difference of 8160 Pa generates a centripetal force. The combined effects of the centripetal force and the tangential velocity generate the most intense swirl as shown in fig. 7.

Volumetric flow rate

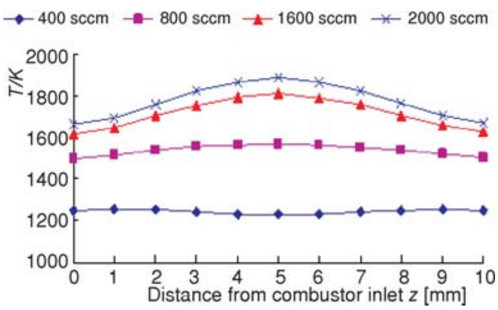

Figure 9. Centerline wall temperature distribution in different flow rates (θ = 20°)

According to the analysis above, the highest average combustion temperature is achieved when the inlet angle is 20°. At this inlet angle, four different volumetric flow rates of 400 sccm, 800 sccm, 1600 sccm, and 2000 sccm are taken to investigate the influence of the flow rate on the combustion process in combustor A. The average wall temperature distribution of the centerline at different flow rates is shown in fig. 9. It indicates that there is an increase in average wall temperature as the flow rate increases. Overall, the curve is smooth, which indicates a uniform temperature distribution.

It can also be observed from fig. 9 that the higher the flow rate is, the less uniform the temperature distribution becomes. This explains why higher temperature has been found at the center of the chamber. It is because the increase of flow rate increases the inlet velocity of the mixed gas, which results in a larger diffusion range inside the combustor and a more intense swirl movement; hence, expanding the effective combustion area for complete combustion. In addition, the more intense swirl leads to the strengthening of the heat transfer rate. In our previous work [27], the centerline wall temperature was measured experimentally in the same dimension with combustor B. Comparing with the numerical results as shown in fig. 9; the centerline wall temperature of combustor B is more sensitive to the changes of inlet flow rates. As the flow rate varies from 400 sccm to 2000 sccm, the highest centerline wall temperature changes from 1210 K to 1880 K, and the temperature difference in our previous work is larger than that in combustor A. Compared to combustor B, a swirl appears in the center of the newly designed combustor A, making the disturbance of the flow more powerful and enhancing the exchange of heat and mass. The benefit of this is the relief of the residence time problem caused by the increasing flow rate, which means that there will not be a sharp reduction of the residence time in combustor A when the flow rate increases. Figure 10 shows the velocity distribution in combustor A at different flow rates. A certain size of swirl appears at the center in each graph, and the size of the swirl expands with the increase of inlet flow rate. At a flow rate of 400 sccm, the diameter of the swirl is about 0.96 mm as shown in fig. 10(a). The diameter of the swirl increases to 1.7 mm when the flow rate increases to 2000 sccm as illustrated in fig. 10(d). The addition of pressure difference and velocity in the combustor results in a bigger swirl. The pressure difference of 975 Pa is recorded near the outlet at the flow rate of 400 sccm, whereas the pressure difference rises to 46000 Pa at the same location at the flow rate of 2000 sccm. The differences

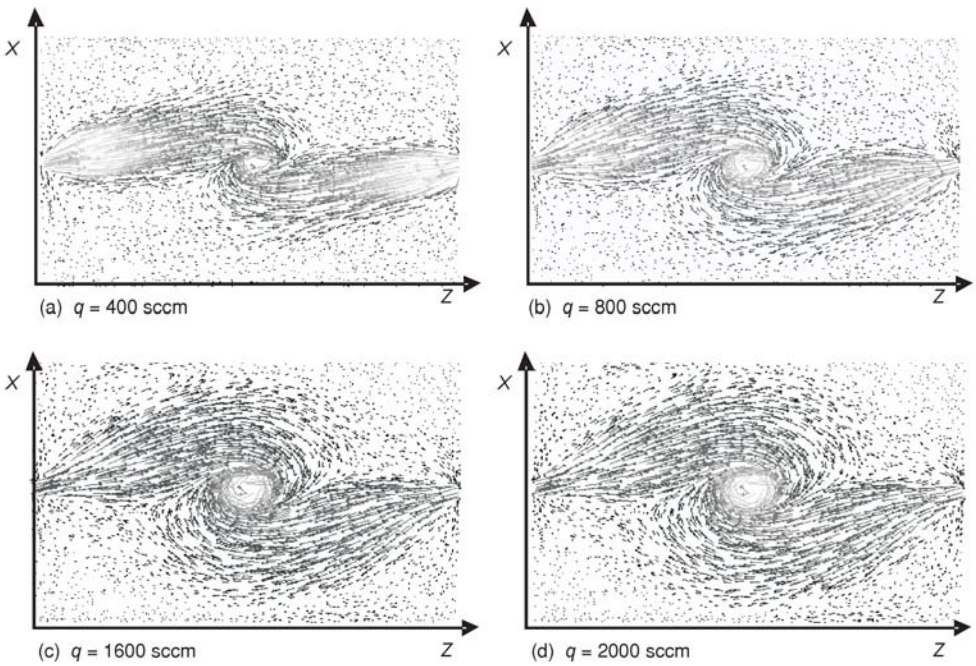

Figure 10. Map of the velocity vectors in different flow rates

between them are so large that the swirl motion becomes more intense, as shown in fig. 10(d), which makes it easier to form a swirl burning near the outlet, resulting in a complete combustion and a higher combustion temperature.

Combustion efficiency

In the conventional combustion technology, combustion efficiency is defined as the ratio of the actual heat released to the maximum heat released. The efficiency of a combustion process can also be defined in a number of ways but is typically described as being either combustion or a destruction efficiency. Combustion efficiency focuses on the fully oxidized combustion products with the goal of completely oxidizing all of the fuel. In the case of hydrogen fuel, this means that all hydrogen must end up as H_2O in order to be 100% efficient. In this paper, the fuel is only hydrogen, so the combustion efficiency used in this work can be defined as the actual H_2O percentage by volume at the outlet, divided by the ideal H_2O percentage by volume at the outlet. So the combustion efficiency can be represented by the equation:

$$\eta = \frac{V_{\mathrm{ihp}}}{V_{\mathrm{ahp}}} \tag{1}$$

where V_{ahp} and V_{ihp} denote the actual H_2O percentage and the ideal H_2O percentage by volume at the outlet, respectively. Figure 11 shows the combined effects of inlet angle and the flow rate on the H_2O percentage by volume at the outlet. It is observed that the H_2O percentage decreases with the increase of flow rate and it increases with the increase of inlet angle.

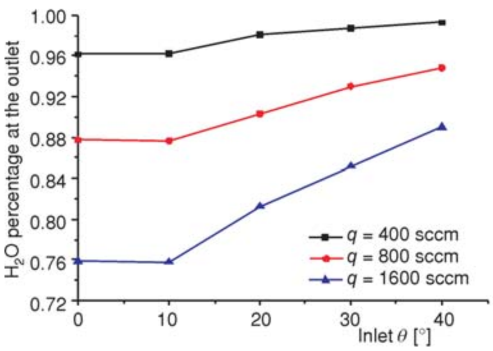

Figure 11. H_2O percentage in different inlet angles and flow rates at the outlet

Increasing inlet flow rate decreases percentage of H_2O because of the change of the internal flow field structure and the fuel residence time. With the increase of flow rate, the flow velocity becomes faster; the fuel residence time actually becomes shorter, which leads to an incomplete combustion at the same inlet angle, therefore, the combustion efficiency decreases as the inlet rate increases. The change of θ also affects the H_2O percentage. It can be seen from fig. 11 that the H_2O percentage at the outlet increases with the increase of inlet angle at the same flow rate. Taking q = 1600 sccm for example, the H_2O percentage is only 76% when the θ = 0° and it increases to 89% when the θ = 40°. A same increasing trend can be seen at the other two flow rates. As can be observed from the fig. 10, the bigger the inlet angle is, the longer the fuel travels in the micro chamber, which means a longer fuel residence time and the enhanced efficiency of combustion.

From this analysis, it can be concluded that the maximum H_2O percentage and the maximum wall temperature are not obtained at the same inlet angle. The maximum average wall temperature is approximately achieved at inlet angle θ = 20° for all flow rates as shown in fig. 6, whereas the highest combustion efficiency is achieved at θ = 40°. This is a very complex process and the values of inlet angles affect the value of the tangential velocity and results in the formation of the swirl motion, which strengthens the disturbance at the boundary layer and the mainstream, and subsequently reducing the thickness of laminar boundary layer and enhancing the heat transfer intensity. Inlet angle of 20° is the best inlet condition for the impact and mixing of the flow, the heat transfer intensity between the fluid zone and the walls is enhanced the most, which results in higher average temperature. Hence, it is not able to simultaneously achieve the maximum H_2O percentage at the outlet and the maximum mean temperature on the wall.

Conclusions

In this paper, a new type of micro-combustor with two-nozzle is proposed. The performance of it is investigated numerically in different inlet angles and different inlet flow rates. The result shows that a swirl is formed in the center of the chamber, which changes the inner flow structure. In addition, the H_2O percentage at the outlet is investigated. The following conclusions have been obtained by numerical simulation.

- From the comparative analysis between the new micro-combustor A and B, the feasibility of the new two-nozzle micro-combustor has been verified. It has a higher and more uniform wall temperature distribution, which is beneficial for the MTPV system.
- At higher inlet flow rates, an intense swirl will emerge in combustor A when $\theta > 10°$. This swirl can enhance the burning intensity. Moreover, the optimum wall temperature distribution is obtained approximately at $\theta = 20°$.
- The maximum combustion efficiency and the maximum mean wall temperature are not simultaneously achieved at the same angle.
- To some extent, the increase in the inlet angle θ affects the fluid field within the combustion chamber and enhances the fluid boundary layer disturbance, and the mixing in the mainstream, resulting in thinner laminar boundary layer and enhancing the heat transfer rate.

Acknowledgments

The authors wish to acknowledge the research grant from National Science Foundation of China (No. 51376082, 51206066, and 51476071), Natural Science grant of Jiangsu province (No. BK20131253) and the Project Funded by the Priority Academic Program Development of Jiangsu Higher Education Institutions (PAPD).

References

[1] Hebling, C., *et al*., Micro-Fuel Cells, *Comprehensive Microsystems, 3* (2008), pp. 613-634
[2] Fernandez-Pello, A. C., Micro-Power Generation Using Combustion: Issues and Approaches, 29th Symposium on Combustion, Sappor, Japan, 2002, *Proceedings*, The Combustion Institute, Pittsburgh, Penn., 2003, pp. 909-916
[3] Epstein, A. H., *et al*., Power MEMS and Microengines, *Proceedings*, International Conference on Solid State Sensors and Actuators, Chicago, Ill., USA, 1997, pp.16-19
[4] Suzuki, Y., *et al*., Experimental Study on Mechanical Power Generation from MEMS Internal Combustion Engine, *Sensors and Actuators A: Physical, 141* (2008), 2, pp. 654-661
[5] Chou, S. K., *et al*., Development of Micro Power Generators – A Review, *Applied Energy, 88* (2011), 1, pp. 1-16
[6] Jacobson, S. A., Epstein, A. H., The International Symposium on Micro-Mechanical Engineering, Tsukuba, Japan, 2003
[7] Maruta, K., Micro and Mesoscale Combustion, 33th Symposium on Combustion, Beijing, China, 2010, *Proceedings*, The Combustion Institute, Pittsburgh, Penn., USA, 2011, 1, pp. 125-150
[8] Epstein, A. H., Senturia, S. D., Macro Power from Micro Machinery, *Science, 276* (1997), p. 1211
[9] Fu, K., *et al.*, Design and Experimental Results of Small-Scale Rotary Engines, *Proceedings*, 2001 ASME International Mechanical Engineering Congress and Exposition, New York, USA, 2001, pp. 259-302
[10] Zhang, S. M., Wang, J. S., A Novel Micro Free-Piston Swing Engine and the Validation of its Feasibility (Part 1), SAE 320021, 2003
[11] Yang, W. M., *et al*., Development of Microthermophotovoltaic System, *Applied Physics Letters, 81* (2002), 27, pp. 5255-5257

[12] Yang, W. M., *et al*., Development of a Prototype Micro-Thermophotovoltaic Power Generator, *Journal of Physics D: Applied Physics, 37* (2004), 7, pp. 1017-1020
[13] Chou, S. K., *et al*., Porous Media Combustion for Micro Thermophotovoltaic System Applications, *Applied Energy, 87* (2010), 9, pp. 2862-2867
[14] Mujeebu, M., *et al*., Applications of Porous Media Combustion Technology – A Review, *Applied Energy, 86* (2009), 9, pp. 1365-1375
[15] Tobler, W., *et al*., High-Performance Selective Er-Doped YAG Emitters for Thermophotovoltaics, *Applied Energy, 85* (2008), 6, pp. 483-493
[16] Qiu, K., Hayden, A. C. S., Development of a Novel Cascading TPV and TE Power Generation System, *Applied Energy, 91* (2012), 1, pp. 304-308
[17] Lloyd, S. A., Weinberg, F. J., Limits to Energy Release and Utilisation from Chemical Fuels, *Nature, 257* (1975), Oct., pp. 367-370
[18] Ronney, P., Analysis of Non-Adiabatic Heat-Recirculating Combustors, *Combustion and Flame, 135* (2003), 4, pp. 421-439
[19] Ju, Y., Choi, C., An Analysis of Sub-Limit Flame Dynamics using Opposite Propagating Flames in Mesoscale Channels, *Combustion and Flame, 133* (2003), 4, pp. 483-493
[20] Wang, H., *et al*., Direct Numerical Simulation and Analysis of a Hydrogen/Air Swirling Premixed Flame in a Micro Combustor, *Int. J. Hydrogen Energy, 36* (2011), 21, pp. 13838-13849
[21] Feng, L., *et al*., Numerical Study of Methane and Air Combustion Inside a Small Tube with an Axial Temperature Gradient at the Wall, *Applied Thermal Engineering, 30* (2010), 17-18, pp. 2804-2807
[22] Khandelwal, B., *et al*., Experimental Studies on Flame Stabilization in a Three Step Rearward, *Applied Thermal Engineering, 58* (2013), 1-2, pp. 363-368
[23] Fan, A. W., *et al*., Effect of Bluff Body Shape on the Blow-Off Limit of Hydrogen/Air Flame in a Planar Micro-Combustor, *Applied Thermal Engineering, 62* (2014), 1, pp. 13-19
[24] Li, J., *et al*., A Numerical Study on Premixed Micro-Combustion of CH_4-Air Mixture: Effects of Combustor Size, Geometry and Boundary Conditions on Flame Temperature, *Chemical Engineering Journal, 150* (2009), 1, pp. 213-222
[25] ***, ANSYS Inc., ANSYS FLUENT Release 14.0, Canonsburg, Penn., USA, 15317, 2011
[26] Miller, J. A., Bowan, C. T., Mechanism and Modeling of Nitrogen Chemistry in Combustion, *Progress in Energy and Combustion Science, 15* (1989), 4, pp. 287-338
[27] Pan, J. F., *et al*., Micro Combustion in Sub-Millimeter Channels for Novel Modular Thermophotovoltaic Power Generators, *Micromech. Microeng, 20* (2010), 12, p. 125021

Paper submitted: November 11, 2014
Paper revised: May 7, 2015
Paper accepted: May 29, 2015